Monitoring of seasonal snow cover in Bhutan using remote sensing technique

Deo Raj Gurung[1,*], Anil V. Kulkarni[2], A. Giriraj[3], Khun San Aung[1] and Basanta Shrestha[1]

[1]International Centre for Integrated Mountain Development, GPO Box 3226, Dhapakhel, Lalitpur, Kathmandu, Nepal
[2]Divecha Centre for Climate Change, Indian Institute of Science, Bangalore 560 012, India
[3]International Water Management Institute, 127, Colombo, Sri Lanka

All major rivers in Bhutan depend on snowmelt for discharge. Therefore, changes in snow cover due to climate change can influence distribution and availability of water. However, information about distribution of seasonal snow cover in Bhutan is not available. The MODIS snow product was used to study snow cover status and trends in Bhutan. Average snow cover area (SCA) of Bhutan estimated for the period 2002 to 2010 was 9030 sq. km, about 25.5% of the total land area. SCA trend of Bhutan for the period 2002–2010 was found to decrease (–3.27 ± 1.28%). The average SCA for winter was 14,485 sq. km (37.7%), for spring 7411 sq. km (19.3%), for summer 4326 sq. km (11.2%), and for autumn 7788 sq. km (20.2%), mostly distributed in the elevation range 2500–6000 m amsl. Interannual and seasonal SCA trend both showed a decline, although it was not statistically significant for all sub-basins. Pho Chu sub-basin with 19.5% of the total average SCA had the highest average SCA. The rate of increase of SCA for every 100 m elevation was the highest (2.5%) in the Pa Chu sub-basin. The coefficient of variance of 1.27 indicates high variability of SCA in winter.

Keywords: Climate change, remote sensing, snow cover, water availability.

SNOW cover is an important natural resource to countries like Bhutan, where hydropower and agriculture constitute two major contributors to the national exchequer, with 22% and 17% share of GDP[1]. Change in the hydrological regime due to changes in snowmelt and snowfall pattern can influence national economy and livelihood of the people. Therefore, monitoring of seasonal snow is important to understand the impact of climate change on water availability for socio-economic development of the country. In addition, information about temporal and spatial distribution of seasonal snow cover is an important indicator of climate monitoring[2,3].

Many recent studies on snow cover variability both at the global[4] and regional[5–8] scale have shown a decline in snow cover area (SCA), particularly in spring season. Large spatial variation in SCA due to altitudinal differences across the Hindu Kush Himalaya (HKH) has been reported[7,9]. Such variability is prominent during the beginning of snow accumulation and ending of snowmelt seasons in Northern Xinjiang, China[10]. The Western Himalaya accounts for higher average snow cover due to higher mean elevation, influence of winter westerlies and northerly latitude[11], resulting in west–east gradient of snow cover[7,11]. However, west–east gradient is subtle during summer, suggesting similar SCA across the Himalaya[10]. Snow cover depletion pattern is important in assessing contribution of snowmelt to hydrological regime of river systems. Different snow-cover peaks have been reported across the HKH region: February in the Western Himalaya[12]; January in Kashmir valley[13] and end of March in Baspa basin[14]. In China, snow peak has been recorded in January for Qinghai-Xizang (Tibet) Plateau and mid-March for western China[8]. In addition, altitude can also influence snow depletion pattern[9].

Information about distribution of seasonal snow cover in Bhutan is not available. Therefore, a study was carried out to monitor seasonal snow cover using Moderate Resolution Imaging and Spectroradiometer (MODIS) data. MODIS data have been used extensively to monitor SCA[7,15–17]. SCA was estimated for 9 years from 2002 to 2010.

Bhutan is a small country with an area of 38,394 sq. km, lodged in the southern slope of the Eastern Himalaya between 26°42′0.66″–28°14′50.40″N lat., and 88°44′55.71″–92°07′40.56″E long. (Figure 1). It is approximately 300 km from east to west and 175 km from north to south. Within the short span of south to north stretch, relief changes from over several metres to over 7000 m amsl. The northern frontier of Bhutan, characterized by a lofty range acts as a barrier for inland-bound monsoon from the Bay of Bengal, resulting in both snow (Higher Himalaya) and rain (mid-Himalaya and the foothills). SCA was analysed for 10 basins of Bhutan (Figure 1).

In this study data from MODIS sensor with spatial resolution of 500 m were used for snow cover assessment. The 8-day composite MODIS snow products from Aqua (MYD10A2) and Terra (MOD10A2) for the period 2002 to 2010 were used to generate an enhanced product as described below. Accuracy assessment of standard MODIS 8-day product in China using *in situ* data showed overall accuracy of 87% and 93% with and without cloud cover[10]. Inter-comparison of cloud-filtered MODIS snow cover product with that from Advance Wide Field Sensor (AWiFS) images using the Indian Remote Sensing Satellite (IRS) resulted[5] in overall accuracy of 93%. However, accuracy depends on land-cover type, timing, season and topography[18].

The snow products were generated by the NASA Goddard Space Flight Center in Greenbelt, MD, USA and made available by the National Snow and Ice Data Center (NSIDC), Colorodo, USA. Snow was mapped using the Normalized Difference Snow Index (NDSI) method, with

*For correspondence. (e-mail: drgurung@icimod.org)

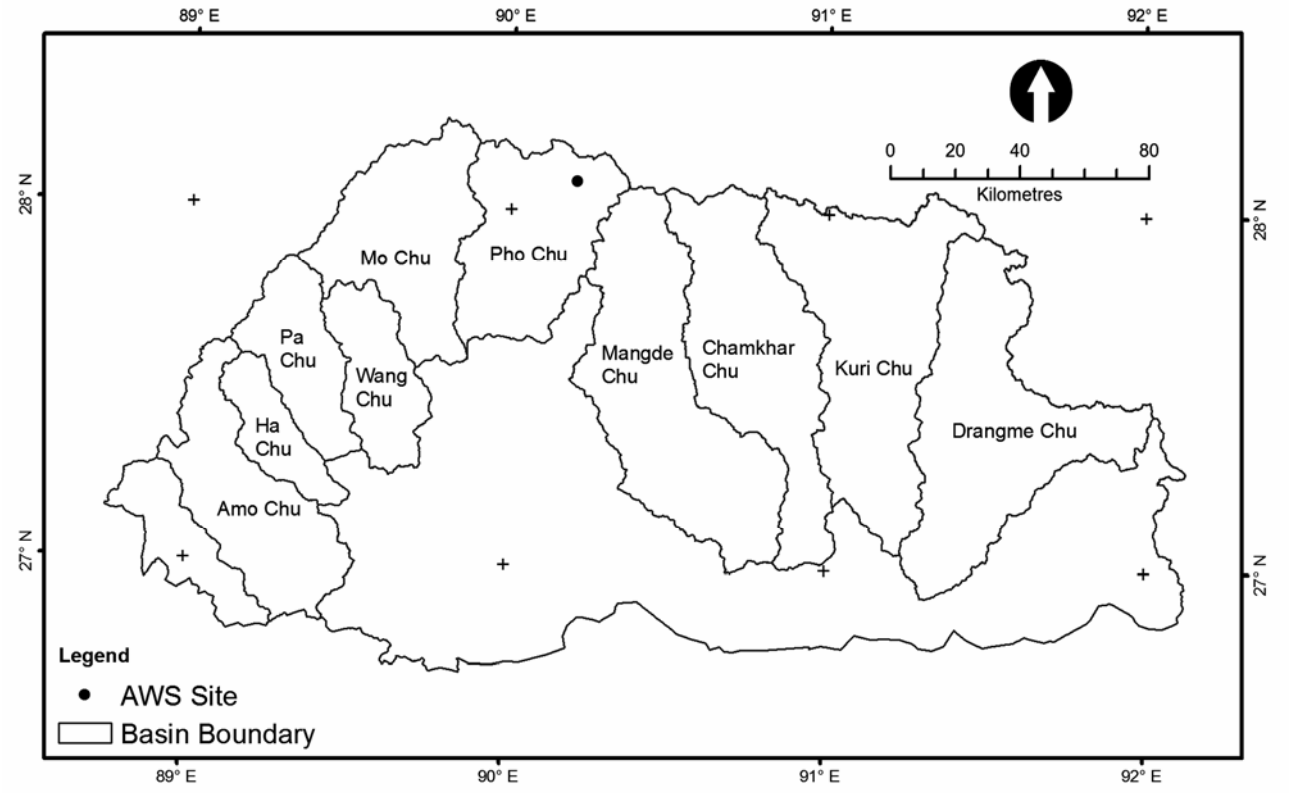

Figure 1. Map of Bhutan showing distribution of sub-basins.

reflectance in bands 4 (0.545–0.565 μm) and 6 (1.628–1.652 μm). The NDSI was calculated using the following relationship[15].

$$\text{NDSI} = (\text{Band 4} - \text{band 6})/(\text{band 4} + \text{band 6}). \quad (1)$$

The 8-day composite MODIS snow products from Aqua (MYD10A2) and Terra (MOD10A2) for the period 2002–2010 were used after improving cloud filtering and removing/cleaning snow pixels from lower altitude.

The elevation data of Shuttle Radar Topography Mission (SRTM) were used to study distribution of snow cover in different elevation zones and aspect. The SRTM Digital Elevation Model (DEM) at 90 m spatial resolution was resampled to 500 m to maintain consistency with snow data. The 500 m SRTM was then used for deriving snow statistics based on topographic parameters.

Air temperature records (°C) for every 30 min interval from 16 October 2003 to 13 August 2010 from an Automatic Weather Station (AWS) located at Tenchoe village (28°04′46.98″N and 90°12′21.98″E) at an altitude of 4109 m amsl, in Lunana (Figure 1) was available. However, data were missing for a considerable time-period (between 8 October 2005 and 4 July 2007).

To achieve consistency with the 8-day MODIS snow-cover products for analysis, air temperature data were processed as the average of the same 8-day period[10].

Cloud cover is a major issue in summer to map snow cover due to continuous overcast conditions. Cloud filtering approach described by Gafurov and Bardossy[19] was implemented. In addition, altitude-based masking was implemented in order to remove misclassified snow pixels found in low altitude.

Time lag in the overpass timing of Terra and Aqua allows us to reclassify cloud pixel in one of the products with information from the corresponding pixel from the other product. This is done by combining Terra and Aqua snow products as explained in eq. (2).

$$S(x, y, t) = \max(\text{SA}(x, y, t), \text{ST}(x, y, t)), \quad (2)$$

where y is the index for row (vertical), x the index for column (horizontal), t the index for day (temporal) of pixel S, and SA and ST are the Aqua and Terra pixels respectively. It had removed ~ 40% of the cloud in case of the HKH region which comprises mainly of mountain areas (from the Hindu Kush range in the west through Karakoram to the Eastern Himalayan range in the east) from eight countries (Afghanistan, Bangladesh, Bhutan, China, India, Myanmar, Nepal and Pakistan).

After combining Terra and Aqua data of 8 days, if any pixel was identified as a cloud, then the temporal filter was applied to identify the land feature below the cloud. Initially the same class as given in backward 8-day pro-

duct was used and subsequently, if the pixel was still identified as a cloud, then forward 8-day product was used. The pixels identified as cloud in all three sets of 8-day products are retained as cloud. The relationship is explained in eq. (3).

$$S(x, y, t) = 1 \text{ if } S(x, y, t-8) = 1 \text{ or } S(x, y, t+8) = 1, \quad (3)$$

where $S-8$, S and $S+8$ are three consecutive sets of 8-day products; 1 corresponds to snow cover, and 0 land cover.

Using this approach, additional ~50% of the cloud pixels were removed by the filter in the case of the HKH region.

Spatial filter works on the basis of majority algorithm, and determines the new value of the cell based on the most popular values within the filter window. The assumption is not always true, but the probability of a pixel having the same cover as the cover with maximum presence is high. This spatial filtering is applied selectively only to the cloud pixel and missing data, whereas the other original data are maintained. After applying temporal filters, a large area was also found under cloud cover and majority of these cloud pixels were observed during the monsoon season. To remove cloud spatial filter was used with 7×7 filter window, which has proved optimal in removing cloud pixels. In the spatial filter, majority of a valid class (but not the cloud class) within 7×7 window was used to replace the cloud or missing data pixel, but not the snow/land pixel. The spatial filtering mostly removes some cloud pixels surrounded by land/snow and some cloud pixels at the edge of the big cloud area. Spatial filter removed additional 5% of the cloud pixels.

Sometimes the global MODIS snow product erroneously classifies pixels as snow in the lower altitude regions of southern Bhutan. Therefore, threshold value of 1000 m was taken to remove such snow pixels. The success of the filter is based on the presence of the misclassified snow pixels.

To automate cloud filtering steps and extraction of snow cover statistics for different terrain aspects (slope, altitude and slope), an image processing and analysis tool was developed. The core program was written in C using free and open source image handling libraries which are distributed under General Public License. A Graphic User Interface was written in Microsoft Visual C# 2008 using Microsoft Visual Studio 2008.

Since Aqua (MYD10A2) product is available from August 2002, SCA analysis was done for 9 years (2002–2010). Annual average SCA was used to study interannul trend. The seasonal SCA trend over time was analysed for winter (November–February), spring (March–May), summer (June–August) and autumn (September–October).

The SCA figures for basins were derived based on enhanced MODIS snow product generated at International Centre for Integrated Mountain Development (ICIMOD), Kathmandu, Nepal. SCA distribution for every 500 m was derived and analysed for studying the relationship between SCA and elevation. Detailed SCA analysis was done for 10 sub-basins (Figure 1) to study inter-basin variation, in addition to analysis at the country level.

Table 1. Mean extent of seasonal snow cover in Bhutan

Season	Snow extent (sq. km)	Snow extent (%)
Winter	14,485	37.7
Summer	4,326	11.2
Spring	7,411	19.3
Autumn	7,788	20.2

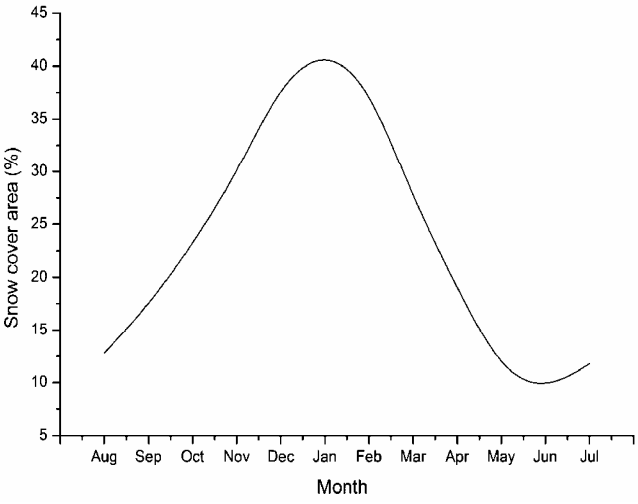

Figure 2. Snow accumulation and ablation curve of Bhutan, based on mean 8-day snow cover for a period between 2000 and 2010.

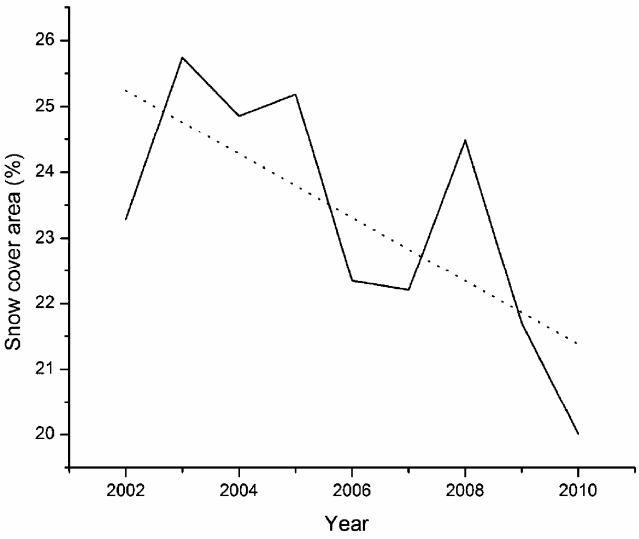

Figure 3. Decadal trend in snow cover of Bhutan from 2000 to 2010. The solid line depicts variation in mean annual SCA, and the dashed line represents linear trend for the decade.

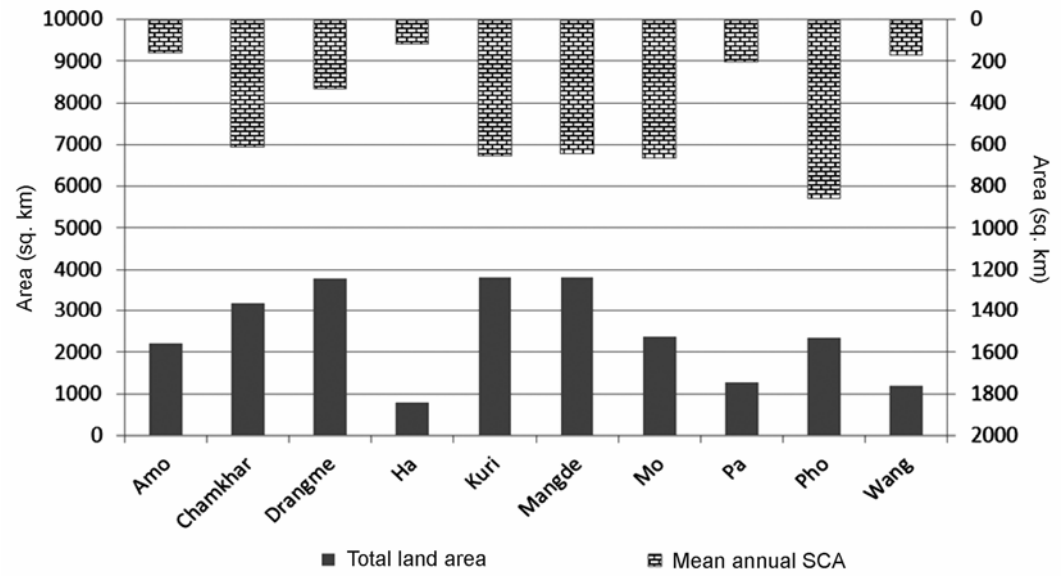

Figure 4. Distribution of snow cover in 10 sub-basins of Bhutan.

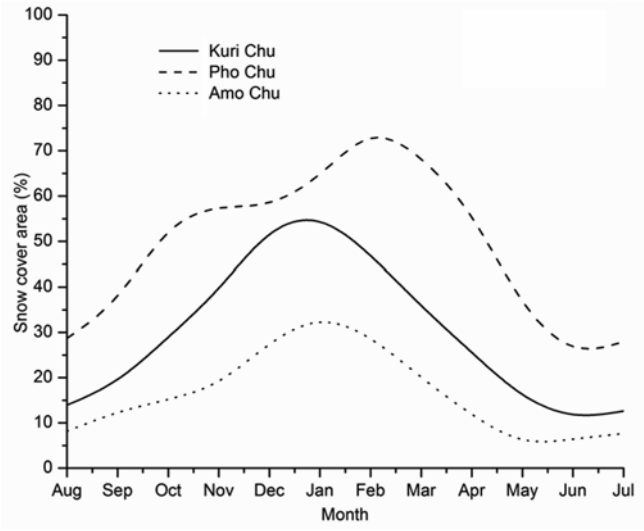

Figure 5. Mean monthly distribution of snow cover in Amo Chu, Kuri Chu and Pho Chu sub-basins of Bhutan.

Comparison of processed 8-day average air temperature from AWS with 8-day SCA of Pho Chu sub-basin was done to understand the relationship.

Average SCA in Bhutan estimated during 2002–2010 was 9030 sq. km, which is 25.5% of the total land area. The mean SCA for different seasons is given in Table 1.

Snow depletion curve suggests that normally snowfall starts in September and during some years as early as August, indicating the role of monsoon precipitation in snow accumulation. However, snow cover remains below 35% till October. Accumulation gradually increases and peaks in February, after which ablation starts, much like in the Kashmir valley[13] and Western Himalaya[12]. The maximum snow extent was observed between 40% and 49% of the total land area. By April, about 50% of the snowmelts (Figure 2). The maximum snow extent was observed in 2004–2005, consistent with the observations in the Western Himalaya[13,20]. The annual snow cover was estimated using 8-day products. The trend of snow cover is plotted in Figure 3 for a period between 2002 and 2010. A declining decadal trend of $-3.27 \pm 1.28\%$ was observed in Bhutan. Winter recorded the highest SCA with 37.7% of the land area under snow and summer with 11.2% of land under snow recorded the least (Table 1). Statistically significant declining trend was observed for spring, consistent with observations in the Western Himalaya[12]. The coefficient of variation (CV) estimated for SCA based on seasons showed high variability for winter (1.27), whereas it was least for summer (0.14). Similarly, it was 0.69 for spring and 0.54 for autumn.

Distribution of snow cover extent was analysed for 10 sub-basins in Bhutan (Figure 4). The highest mean annual SCA of 857 sq. km which constitutes 19.5% of the total land area was observed in the Pho Chu basin. The lowest mean annual SCA of 114 sq. km was observed in the Ha Chu basin. Annual trend of mean SCA for the last 9 years (2002–2010) was analysed for 10 sub-basins and it was largely found to decline.

The snow accumulation and ablation curves differ for each sub-basin, depending upon climatologically sensitive zones and altitude distribution of the basin[17]. Snow accumulation and ablation characteristics for three sub-basins, Amo Chu, Pho Chu and Kuri Chu, spread across (west to east) Bhutan was analysed (Figure 5). All three sub-basins are different in terms of land area (Figure 4) and elevation range. The Pho Chu sub-basin with much of the area above 3500 m, clearly show two SCA peaks (Figure 5), in November and February. The Amo Chu and Kuri Chu sub-basins with lower elevation range (large area below 4000 m) indicate only subtle sense of

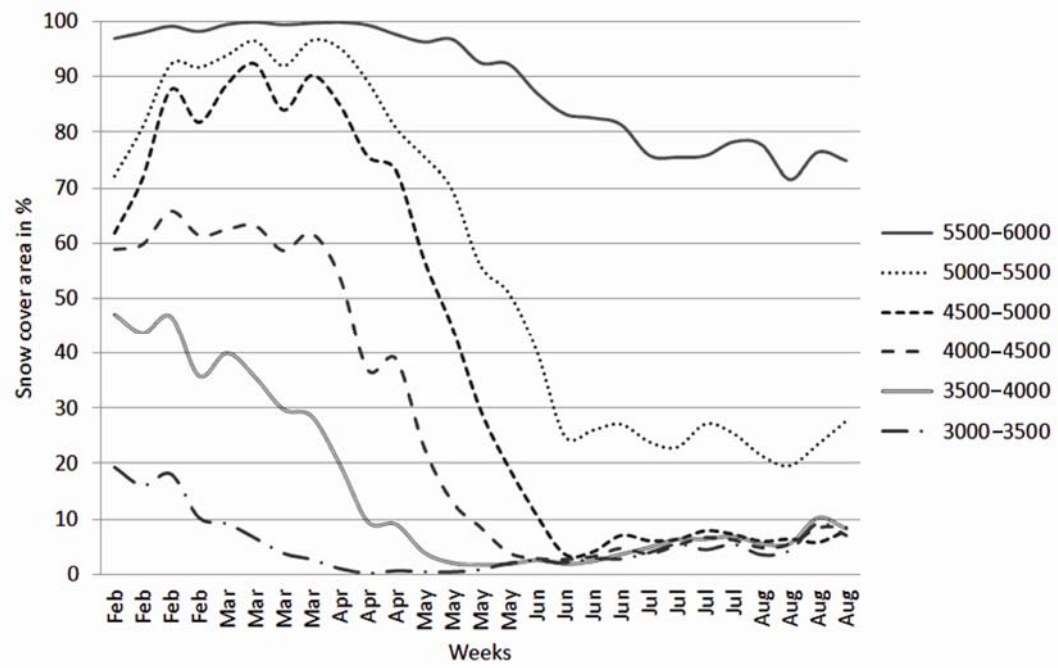

Figure 6. Snow depletion curve for Mangde Chu sub-basin for altitudes above 3000 m for every 500 m.

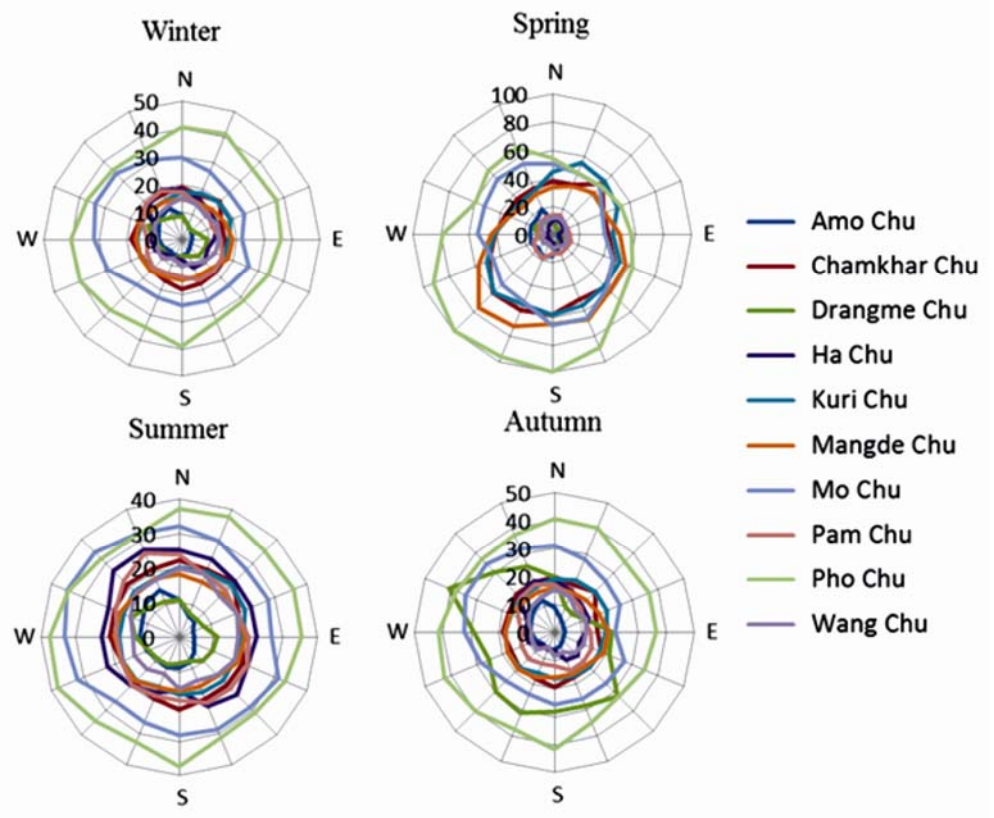

Figure 7. Effect of orientation on distribution of snow cover.

subsidiary peak in October. Difference in peak time and depletion rate was also observed. The Kuri Chu sub-basin was seen to peak in January followed by slower depletion phase, whereas the Pho Chu and Amo Chu sub-basins were seen to peak a month later in February followed by much faster depletion phase.

Elevation can influence snow accumulation due to orography temperature decreasing with increasing height[21].

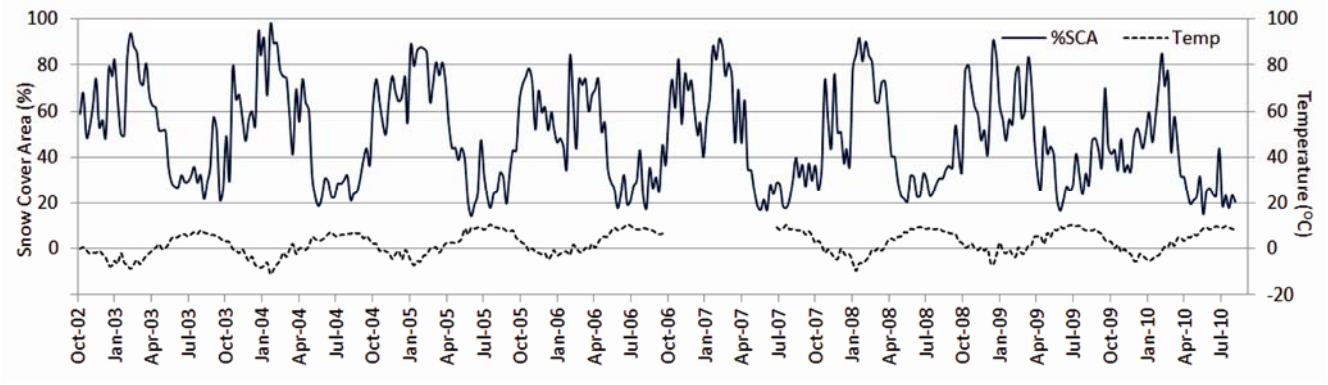

Figure 8. Comparison of 8-day snow cover area (dashed line) and average air temperature (solid line) for the same time-period.

Rate of increase of SCA for every 100 m elevation for all 10 sub-basins was evaluated from a linear plot between elevation and SCA. This was comparable with the Western Himalaya[21]. It was highest (2.5%) for Pa Chu sub-basin and lowest (0.9%) for Amo Chu sub-basin. The coefficient of variance of 1.27 indicates high variability of SCA in winter. The snow depletion curve for an altitude range between 3000 and 6000 m at an interval of 500 m for Mangde Chu sub-basin is plotted in Figure 6. The mean depletion curve was generated using 9 years 8-day snow-cover products. The graph suggests different snowmelt periods for different time intervals in summer. This would be an important input for snowmelt run-off modelling.

Figure 7 shows snow distribution based on orientation of the slope. Contrary to the situation in the Western Himalaya[21], northeast and southwest facing slopes seem to be conducive for snow accumulation (during winter, summer and autumn) in Bhutan. As the days warm up in spring, melting intensifies particularly in northeast and northwest facing slopes, thus drastically reducing the SCA.

Although temperature data available from the AWS at Lunana did not yield significant trend: $+0.04 \pm 4.70$°C (October 2002–September 2006) and $+0.01 \pm 5.00$°C (July 2007–September 2010), they revealed increasing tendency. A study in the Upper Indus using the Climate Research Unit (CRU) dataset has shown that the rate (per year) of increase in air temperature is higher for higher elevation[7]. Overall SCA has an inverse relationship with mean air temperature (Figure 8), consistent with a similar study in China[9]. There seems to be certain time lag before the SCA peak after the minimum mean air temperature (Figure 8). There exists good correlation between SCA and air temperature ($R^2 = 0.62$), which has also been reported from China[10]. The level of correlation (R^2) was found to vary with air temperature: 0.19 for < –5°C, 0.003 for –5°C to 0°C, 0.34 for 0°C to 5°C, and 0.19 for 5°C to 10°C. The slope of the liner plot which explains the response of SCA to temperature, indicates rapid response for the temperature range between 0°C and 5°C (slope = –6.68).

This article describes snow cover status and trend in Bhutan based on the MODIS 8-day snow product. Over a quarter of the total land area of Bhutan remains under snow in winter, which has been decreasing over this decade as indicated by the declining trend. Interannual trend and seasonal trend for SCA in Bhutan from 2002 to 2010 is also showing a decline. In conformity with the Western Himalaya, snow cover in spring is decreasing. The good correlation between SCA and air temperature strongly supports that the decline in SCA is due to increase in mean air temperature. Thus the increasing air temperature, more prominent in the high-altitude belt, will have an impact on SCA and river hydrology with severe, long-term consequences on hydropower generation and agricultural productivity.

It is important to monitor snow cover at a longer time horizon for assessing water resources, as well as for larger-scale global environment monitoring. Clearly, a longer time series of data is needed to attain any definitive conclusions, made feasible by deploying remote sensing techniques in conjunction with field-based, *in situ* data.

1. Asian Development Bank, Asian development outlook 2010: macroeconomic management beyond the crisis, 2010, p. 283.
2. Arndt, D. S., Baringer, M. O. and Johnson, M. R., State of the climate in 2009. *Am. Meteorol. Soc*., 2010, **91**, S1–S222.
3. Robinson, D. A., Dewey, K. F. and Heim, R. R., Global snow cover monitoring: an update. *Bull. Am. Meteorol. Soc.*, 1993, **74**(9), 1689–1696.
4. Brown, R. D. and Robinson, D. A., Northern hemisphere spring snow cover variability and change over 1922–2010 including an assessment of uncertainty. *Cryosphere*, 2011, **5**(1), 219–229.
5. Gurung, D. R., Kulkarni, A. V., Giriraj, A., Aung, K. S., Shrestha, B. and Srinivasan, J., Changes in seasonal snow cover in Hindu Kush-Himalayan region. *Cryosphere Discuss*, 2011, **5**, 755–777.
6. Menon, S., Koch, D., Beig, G., Sahu, S., Fasullo, J. and Orlikowski, D., Black carbon aerosols and the third polar ice cap. *Atmos. Chem. Phys.*, 2010, **10**, 4559–4571.

7. Immerzeel, W. W., Droogers, P., de Jong, S. M. and Bierkens, M. F. P., Large-scale monitoring of snow cover and runoff simulation in Himalayan river basins using remote sensing. *Remote Sensing Environ.*, 2009, **113**(1), 40–49.
8. Dahe, Q., Shiyin, L. and Peiji, L., Snow cover distribution, variability, and response to climate change in western China. *J. Climate*, 2006, **19**, 1820–1833.
9. Pu, Z., Xu, L. and Salomonson, V., MODIS/Terra observed seasonal variations of snow cover over the Tibetan Plateau. *Geophys. Res. Lett.*, 2007, **34**, 1–6.
10. Wang, X., Xie, H. and Liang, T., Evaluation of MODIS snow cover and cloud mask and its application in Northern Xinjiang, China. *Remote Sensing Environ.*, 2008, **112**, 1497–1513.
11. Bookhagen, B. and Burbank, D. W., Toward a complete Himalayan hydrological budget: spatiotemporal distribution of snowmelt and rainfall and their impact on river discharge. *J. Geophys. Res.*, 2010, **115**, 1–25.
12. Kripalani, R. H., Kulkarni, A. and Sabade, S. S., Western Himalayan snow cover and Indian monsoon rainfall: A re-examination with INSAT and NCEP/NCAR data. *Theor. Appl. Climatol.*, 2003, **74**(1), 1–18.
13. Negi, H., Thakur, N., Kumar, R. and Kumar, M., Monitoring and evaluation of seasonal snow cover in Kashmir valley using remote sensing, GIS and ancillary data. *J. Earth System Sci.*, 2009, **118**(6), 711–720.
14. Kaur, R., Saikumar, D., Kulkarni, A. V. and Chaudhary, B. S., Variations in snow cover and snowline altitude in Baspa Basin. *Curr. Sci.*, 2009, **96**, 1255–1258.
15. Tekeli, A. E., Akyurek, Z., ArdaSorman, A., Sensoy, A. and Unal-Sorman, A., Using MODIS snow cover maps in modeling snowmelt runoff process in the eastern part of Turkey. *Remote Sensing Environ.*, 2005, **97**(2), 216.
16. Terzago, S., Cassardo, C., Cremonini, R. and Fratianni, S., Snow precipitation and snow cover climatic variability for the period 1971–2009 in the southwestern Italian Alps: The 2008–2009 snow season case study. *Water*, 2010, **2**(4), 773–787.
17. Zhang, Y., Yan, S. and Lu, Y., Snow cover monitoring using MODIS data in Liaoning Province, Northeastern China. *Remote Sensing*, 2010, **2**(3), 777–793.
18. Hall, D. K. and Riggs, G. A., Accuracy assessment of the MODIS snow products. *Hydrol. Process.*, 2007, **21**(12), 1534–1547.
19. Gafurov, A. and Bardossy, A., Cloud removal methodology from MODIS snow cover product. *Hydrol. Earth Syst. Sci.*, 2009, **13**(7), 1361–1373.
20. Kulkarni, A. V., Rathore, B. P., Singh, S. K. and Ajai, Distribution of seasonal snow cover in central and western Himalaya. *Ann. Glaciol.*, 2010, **54**, 123–128.
21. Jain, S., Goswami, A. and Saraf, A., Role of elevation and aspect in snow distribution in Western Himalaya. *Water Resour. Manage.*, 2009, **23**(1), 71–83.

ACKNOWLEDGEMENTS. This article is based on work supported by the Swedish International Development Cooperation Agency under the project. The temperature data from AWS data at Lunana, were made available by Karma Toeb, Department of Geology and Mines, Government of Bhutan. We thank our colleagues at ICIMOD, professionals from collaborating institutions, and independent experts who contributed significantly during various parts of the project. We also thank Gauri Dangol and Pradeep Dangol (ICIMOD) for help in analysing snow cover data and graphics work.

Received 26 September 2011; revised accepted 4 October 2011

Does carbonate ion control planktonic foraminifera shell calcification in upwelling regions?

Sushant S. Naik*, Shital P. Godad and P. Divakar Naidu

National Institute of Oceanography, Dona Paula, Goa 403 004, India

Planktonic foraminifera shell weights have been recognized as possible proxy for surface water carbonate ion concentration [$CO_3^{=}$] and atmospheric CO_2. However, to utilize this proxy, it is important to understand whether shell weights truly reflect surface water [$CO_3^{=}$]. We utilize shell weights of *Globigerina bulloides* and *Globigerinoides ruber* in the size range of 300 to 355 μm from a sediment core recovered from above the lysocline in the upwelling region of western Arabian Sea. Shell weights of *G. ruber* and *G. bulloides* show significant correlation with their shell size from recent to 16 kyr, which suggests that shell calcification was controlled by optimum growth conditions. On the other hand, during 16 to 22 kyr, there is no correlation between shell weights and shell size. However, shell weights of *G. bulloides* exhibit significant negative correlation with annual sea surface temperature which suggests that *G. bulloides* calcification might have been controlled by surface water [$CO_3^{=}$]. Therefore it is suggested here that shell weights of *G. ruber* and *G. bulloides* cannot be utilized to reconstruct surface water [$CO_3^{=}$] in this region.

Keywords: Planktonic foraminifera, shell weights, upwelling, western Arabian Sea.

THE atmospheric carbon dioxide (CO_2) has fluctuated between ~180 and 280 ppm between the glacials and interglacials respectively[1]. This atmospheric CO_2 is known to dissolve in surface seawater through physical–chemical reactions and affect the equilibrium between the 'dissolved inorganic carbon (DIC)' species; H_2CO_3, HCO_3^- and $CO_3^{=}$. As CO_2 is absorbed by the ocean, it subsequently causes an increase in [H^+], i.e. lowered pH and a decrease in carbonate ion concentration [$CO_3^{=}$], which makes the seawater less alkaline. Lower seawater [$CO_3^{=}$] is known to reduce the calcification rates of calcite-secreting organisms such as foraminifera[2]. Planktonic foraminifera shell calcification and hence shell weights depend upon [$CO_3^{=}$] of surface waters wherein they calcify[3,4]. Drawing upon this trait, the shell weights of *G. sacculifer* were used to reconstruct [$CO_3^{=}$] of surface waters in the Arabian Sea[5].

The western Arabian Sea is a region of intense upwelling which makes it a strong CO_2 source to the atmosphere in the past and present. However, the CO_2 concentrations

*For correspondence. (e-mail: sushant@nio.org)